

# Inhibition and Alternate Substrate Studies on the Mechanism of Carbapenam Synthetase from *Erwinia carotovora*<sup>†</sup>

Barbara Gerratana, Anthony Stapon, and Craig A. Townsend\*

Department of Chemistry, The Johns Hopkins University, 3400 North Charles Street, Baltimore, Maryland 21218

Received March 6, 2003; Revised Manuscript Received May 3, 2003

**ABSTRACT:** The *Erwinia carotovora* *carA*, *carB*, and *carC* gene products are essential for the biosynthesis of (5*R*)-carbapen-2-em-3-carboxylic acid, the simplest carbapenem  $\beta$ -lactam antibiotic. CarA (hereafter named carbapenam synthetase) has been proposed to catalyze formation of (3*S*,5*S*)-carbapenam-3-carboxylic acid from (2*S*,5*S*)-5-carboxymethyl proline based on characterization of the products of fermentation experiments in *Escherichia coli* cells transformed with pET24a/*carB* and pET24a/*carAB*, and on sequence homology to  $\beta$ -lactam synthetase, an enzyme that catalyzes formation of a monocyclic  $\beta$ -lactam ring with concomitant ATP hydrolysis. In this study, we have purified recombinant carbapenam synthetase and shown in vitro that it catalyzes the ATP-dependent formation of (3*S*,5*S*)-carbapenam-3-carboxylic acid from (2*S*,5*S*)-5-carboxymethyl proline. The kinetic mechanism is Bi–Ter where ATP is the first substrate to bind followed by (2*S*,5*S*)-5-carboxymethyl proline and PPi is the last product released based on initial velocity, product and dead-end inhibition studies. The reactions catalyzed by carbapenam synthetase with different diastereomers of the natural substrate and with alternate  $\alpha$ -amino diacid substrates were studied by HPLC, ESI mass spectrometry, and steady-state kinetic analysis. On the basis of these results, we have proposed a role for each moiety of (2*S*,5*S*)-5-carboxymethyl proline for binding to the active site of carbapenam synthetase. Coupled enzyme assays of AMP and pyrophosphate release in the reactions catalyzed by carbapenam synthetase with adipic and glutaric acid, which lack the  $\alpha$ -amino group, in the presence and absence of hydroxylamine support the formation of an acyladenylate intermediate in the catalytic cycle.

In the late 1970s, the discovery of thienamycin (*I*) led the way to the isolation of over 50 members of a new class of  $\beta$ -lactam antibiotics, the carbapenems. Their basic chemical structure comprises a  $\beta$ -lactam ring fused to an unsaturated five-membered ring that contains no heteroatom at the C-1 position seen in penicillin and cephalosporin. The carbapenems stand out among the  $\beta$ -lactam antibiotics for their broad antibiotic activity and their resistance to most  $\beta$ -lactamases (2). They have been isolated from various species of streptomycetes, and from Gram-negative bacteria such as *Serratia* sp. ATCC 39006 and *Erwinia carotovora* that produce the simplest carbapenem, (5*R*)-carbapen-2-em-3-carboxylic acid (3).

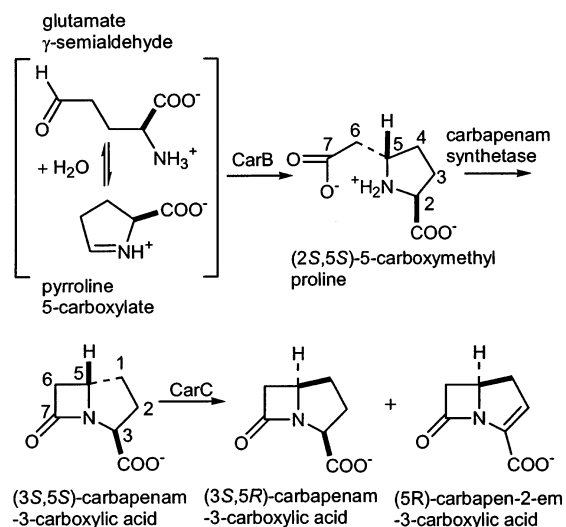
To date, none of the gene clusters responsible for the biosynthesis of carbapenems in streptomycetes has been identified. The genes encoding the (5*R*)-carbapen-2-em-3-carboxylic acid biosynthetic enzymes have been cloned from both *Serratia* sp. ATCC 39006, and *E. carotovora* (4, 5), in addition to a similar gene cluster responsible for the production of an unknown carbapenem-like metabolite from *Photobacterium luminescens* (6). Genetic disruption experiments in *Escherichia coli* transformed with the gene cluster from *E. carotovora* demonstrated that of the nine opening reading frames (ORFs), *carA-H*, only the first five, *carA-E*, encode the enzymes of the biosynthetic pathway to (5*R*)-carbapen-2-em-3-carboxylic acid (7). The products of *carA-C*

are absolutely required for the biosynthesis of this carbapenem from primary metabolites present in *E. coli* (7, 8). Sequence homology of CarD with proline dehydrogenases and incorporation studies with labeled L-proline indicate that the immediate primary metabolite precursor is likely pyrroline-5-carboxylate/glutamate  $\gamma$ -semialdehyde (9). A biosynthetic rationale for the reactions catalyzed by CarA–C has been proposed based on characterization of the products of fermentation experiments in *E. coli* cells transformed with the expression plasmids pET24a/*carABC*, pET24a/*carAB*, or pET24a/*carB* (8) (Scheme 1). CarC shows modest similarity to  $\alpha$ -ketoglutarate dependent non-heme iron oxygenases, and has been demonstrated in vitro to catalyze carbapenem formation from (3*S*,5*S*)-carbapenam-3-carboxylic acid (9). On the basis of the sequence homology of CarA (hereafter named carbapenam synthetase) to  $\beta$ -LS,<sup>1</sup> carbapenam synthetase was proposed to catalyze  $\beta$ -lactam ring formation of the significantly strained carbapenem in a manner similar to  $\beta$ -LS by coupling cyclization to ATP hydrolysis (8).

<sup>1</sup> Abbreviations: IPTG, isopropyl  $\beta$ -D-thiogalactopyranoside; DTT, dithiothreitol; EDTA, ethylenediaminetetraacetic acid; PMSF, phenylmethanesulfonyl fluoride; Tris-HCl, tris(hydroxymethyl)aminomethane hydrochloride; MOPS, 3-(*N*-morpholino)-propanesulfonic acid; CMP, (2*S*,5*S*)-5-carboxymethyl proline; (2*S*,5*R*)-CMP, (2*S*,5*R*)-5-carboxymethyl proline; (2*R*,5*R*)-CMP, (2*R*,5*R*)-5-carboxymethyl proline; carbapenam, (3*S*,5*S*)-carbapenam-3-carboxylic acid; CEP, (2*S*,5*S*)-5-carboxymethyl proline; PPi, pyrophosphate; ESI-MS, electrospray ionization mass spectrometry; DMAP, 4-(dimethylamino)pyridine; brine, saturated sodium chloride solution;  $\beta$ -LS,  $\beta$ -lactam synthetase; AS-B, asparagine synthetase.

<sup>†</sup> This research was supported by NIH Grant AI 14937.

\* To whom correspondence should be addressed. Phone: (410) 516-7444. Fax: (410) 261-1233. E-mail: ctownsend@jhu.edu.

Scheme 1: (5*R*)-Carbapen-2-em-3-carboxylic Acid Biosynthetic Pathway

To understand the mechanism of the ATP-dependent  $\beta$ -lactam ring formation, we have purified recombinant carbapenam synthetase and gathered evidence for the first time in vitro that it catalyzes the biosynthesis of the carbapenam from CMPr in the presence of ATP/Mg<sup>2+</sup>. We have characterized the steady-state kinetic mechanism of carbapenam synthetase based on initial velocity, product and dead-end inhibition studies. The steady-state kinetic parameters have been measured with a variety of substrates to gain insight into the topology of the substrate-binding site of this enzyme giving particular attention to the stereochemical requirements of the substrate. Finally, we report studies of the reactions catalyzed by carbapenam synthetase with diacids as alternate substrates that support the formation of an acyladenylate intermediate.

## EXPERIMENTAL PROCEDURES

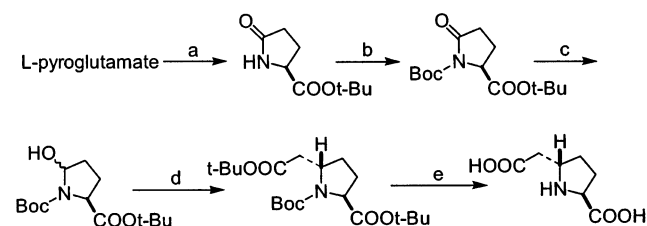
**Materials.** Nondenatured protein molecular weight marker kit, L-aminoadipic acid, L-pyrroglutamic acid, pimelic acid, all buffers, all resins, and all coupling enzymes were obtained from Sigma (St. Louis, MO). Plasmid pET24a/carA was a generous gift from Dr. Rongfeng Li of this laboratory (8). 3-(Carboxymethylamino)-propionic acid was a generous gift from Dr. Fumitaka Kudo of this laboratory. 6-Oxo-piperidine-2-carboxylic acid was prepared by cyclization of L-aminoadipic acid by the method of Akasaka et al. (10). Glutaric acid, adipic acid, D,L-aminopimelic acid, and L-glutamic acid were purchased from Lancaster Synthesis Inc. (Windham, NH), while D-aminoadipic acid, 5-aminovaleric acid, and 6-aminocaproic acid and all the reagents used in the chemical syntheses were from Aldrich (Milwaukee, WI). Pure N-terminal His<sub>6</sub> tagged CarC was overexpressed as described below for recombinant CarC and purified under anaerobic conditions by affinity chromatography with a Ni-NTA column from Qiagen using standard procedures (Valencia, CA) (unpublished experiments).

**Methods.** The carbapenam synthetase extinction coefficient was calculated by performing quantitative amino acid analysis (AAA Laboratory, Merce Island, WA) on triplicate samples with measured  $A_{280}$  values. The quaternary structure

and the molecular weight of native carbapenam synthetase was determined by native discontinuous electrophoresis using the molecular weight marker kit to generate a Ferguson plot as described in the technical bulletin no. MKR-137 from Sigma. Tetrahydrofuran was distilled from sodium/benzophenone ketyl; acetonitrile and methylene chloride were distilled from CaH<sub>2</sub>. Flash chromatography was performed on a 6.5  $\times$  18 cm column packed with Bodman Industries silica gel (230–400 mesh ATM). Melting points are uncorrected. Optical rotations were recorded on a Jasco model P-1010 polarimeter. NMR spectra were obtained on a Varian UnityPlus 400 spectrometer. NMR spectra recorded in CDCl<sub>3</sub> are reported in ppm ( $\delta$ ) downfield from Me<sub>4</sub>Si (<sup>1</sup>H) or relative to CDCl<sub>3</sub> at 77.0 ppm (<sup>13</sup>C). NMR spectra recorded in D<sub>2</sub>O are reported in ppm ( $\delta$ ) relative to D<sub>2</sub>O 4.80 ppm (<sup>1</sup>H) or relative to dioxane at 66.0 ppm (<sup>13</sup>C). All the amino diacids are numbered following standard amino acid nomenclature. The carbapenam is numbered according to the  $\beta$ -lactam antibiotic convention (11).

**Overexpression, Purification, and Characterization of Carbapenam Synthetase.** BL21(DE3) cells were transformed with pET24a/carA and grown at 37 °C in 2 $\times$  YT medium supplemented with 50  $\mu$ g/mL kanamycin A. The cells were induced (OD<sub>600</sub> = 0.65) with 1 mM IPTG at 30 °C, harvested by centrifugation 3 h post-induction, and frozen as a pellet in liquid nitrogen. Usually 12 g of cells were obtained from 3 L of medium. All purification procedures were carried out on ice or at 4 °C. The frozen cells (14 g) were resuspended to 0.3 g/mL in ice-cold lysis buffer (100 mM Tris HCl, pH 8.0, 1.8 mM EDTA, 1 mM PMSF, 1 mM DTT) and broken by French Press at 12000 psi. After removal of the cell debris by centrifugation, streptomycin sulfate was added to a final concentration of 3%. The supernatant obtained by centrifugation was subjected to ammonium sulfate fractionation at 35 and 65% saturation. The pellet from the 65% cut was resuspended in 25 mL of dialysis buffer (50 mM Tris HCl, pH 7.5, 10  $\mu$ M EDTA, 1 mM benzamidine, 1 mM DTT, 1 mM PMSF) and was dialyzed against 3 L of dialysis buffer with two buffer changes in 12 h. The dialyzed suspension was loaded at 3 mL/min on a Q Sepharose FF column (2.5  $\times$  33 cm) preequilibrated with 50 mM Tris HCl, pH 7.5, 1 mM DTT, and 100 mM NaCl. After washing the column with 50 mM Tris HCl, pH 7.5, 1 mM DTT, 100 mM NaCl, the enzyme was eluted with a linear gradient of NaCl in 50 mM Tris HCl, pH 7.5, 1 mM DTT. Fractions containing carbapenam synthetase were pooled and dialyzed against 20 mM MOPS, pH 7.5, 1 mM DTT and concentrated by ultrafiltration in an Amicon stirred cell over a YM10 membrane. The concentrated solution was loaded on a Sephacryl S200HR column (1.2  $\times$  100 cm) equilibrated with 20 mM MOPS, pH 7.5, 1 mM DTT. Carbapenam synthetase was eluted with the same buffer and was again pooled based on SDS-PAGE analysis of the column fractions. The enzyme was concentrated to 10 mg/mL by ultrafiltration and delivered dropwise into liquid nitrogen and stored at –80 °C. Protein concentration was measured spectrophotometrically at 280 nm using the extinction coefficient determined for carbapenam synthetase [ $\epsilon_{280}$  = 1.82 ( $\pm$ 0.16) mL mg<sup>–1</sup> cm<sup>–1</sup> (pH 7.0, 25 °C)].

**Syntheses of Alternate Substrates.** The characterizations of each intermediate in the syntheses of alternate substrates are reported in the Supporting Information.

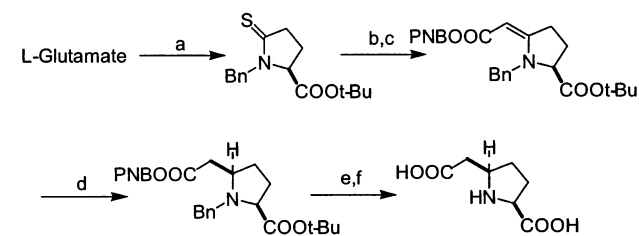
Scheme 2: Synthesis of (2*S*,5*S*)-5-Carboxymethyl Proline<sup>a</sup>

<sup>a</sup> (a) *tert*-Butyl acetate, perchloric acid, 2 d. (b) (Boc)<sub>2</sub>=O, triethylamine, DMAP, CH<sub>3</sub>CN, 1 d. (c) Superhydride, THF, 20 min. (d) *tert*-butyl diethylphosphonoacetate, potassium hydride, DMF, 1 h. (e) trifluoroacetic acid.

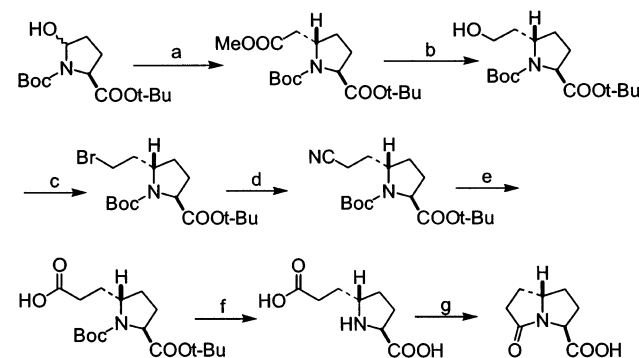
(A) *Synthesis of (2S,5S)-5-Carboxymethyl Proline (Scheme 2).* *tert*-Butyl L-pyroglutamate was prepared according to a published procedure (12, 13) and converted to *tert*-butyl *N*-Boc-5-hydroxy-L-prolinate (14). (2*S*,5*S*) *N*-Boc 5-*tert*-butoxycarbonylmethyl proline *tert*-butyl ester was prepared according to a published procedure (15). *tert*-Butyl diethyl phosphonoacetate (4.55 mL, 19.4 mmol) was added dropwise to a stirring suspension of 30% KH/mineral oil (2.59 g, 19.4 mmol) in 72 mL of dry DMF under an argon atmosphere. After the sample was stirred at room temperature for 1 h, the *tert*-butyl *N*-Boc-5-hydroxy-L-prolinate (4.65 g, 16.2 mmol) in 50 mL of dry DMF was added and the reaction stirred overnight. After aqueous work up, the residue was purified by silica gel chromatography (hexane) to yield a white solid, which was recrystallized from boiling hexane (5.12 g, 13.3 mmol, 82% yield) and deprotected with trifluoroacetic acid. <sup>1</sup>H NMR analysis showed no trace of the (2*S*,5*R*) diastereomer indicating ≥95% purity, a small improvement on the literature (15): 146 mg, 0.84 mmol, 65% yield; mp 206–209 °C; [α]<sub>D</sub><sup>25</sup> –44.6° (c 1, H<sub>2</sub>O). <sup>1</sup>H NMR: δ 4.22 (t, *J* = 8.0 Hz, 1H), 4.05 (p, *J* = 6.8 Hz, 1H), 2.80 (m, 2H), 2.47 (m, 1H), 2.28 (m, 1H), 2.06 (m, 1H), 1.82 (m, 1H); <sup>13</sup>C NMR: δ 173.8, 173.4, 60.2, 56.1, 35.2, 29.2, 27.6; IR: 3185, 2565, 1667, 1610, 1538, 1198 cm<sup>–1</sup>; HRMS calcd for C<sub>7</sub>H<sub>11</sub>NO<sub>4</sub> [M+H<sup>+</sup>]: 174.0761, found 174.0757.

(B) *Synthesis of (2R,5R)-5-Carboxymethyl Proline.* (2*R*,5*R*)-CMPr was prepared as described above for the synthesis of CMPr using as starting material D-glutamic acid: mp 206–209 °C; [α]<sub>D</sub><sup>25</sup> +44.9° (c 1, H<sub>2</sub>O). <sup>1</sup>H NMR: δ 4.20 (t, *J* = 8.4 Hz, 1H), 4.00 (p, *J* = 6.4 Hz, 1H), 2.82 (m, 2H), 2.42 (m, 1H), 2.24 (m, 1H), 2.02 (m, 1H), 1.76 (m, 1H); <sup>13</sup>C NMR: δ 173.7, 173.2, 60.1, 56.1, 35.1, 29.2, 27.6; IR: 3180, 2563, 1669, 1614, 1538, 1199 cm<sup>–1</sup>; HRMS calcd for C<sub>7</sub>H<sub>11</sub>NO<sub>4</sub> [M+H<sup>+</sup>]: 174.0761, found 174.0756.

(C) *Synthesis of (2S,5R)-5-Carboxymethyl Proline (Scheme 3).* *N*-Benzyl-(2*S*)-5-(*p*-nitrobenzyloxycarbonyl)methylidene)-proline *tert*-butyl ester (16) (5.3 g, 11.7 mmol, 86% yield). *N*-benzyl-(2*S*,5*R*)-(p-nitrobenzyloxycarbonyl)methyl)-proline *tert*-butyl ester was synthesized following an established procedure to favor the 5*R* isomer (16). The fully protected vinylogous amide (4.0 g, 8.9 mmol) in dry acetonitrile (80 mL) under argon was reduced with sodium cyanoborohydride (2.23 g, 35.5 mmol). After addition of acetic acid (7.1 mL), the solution was stirred for 20 h and

Scheme 3: Synthesis of (2*S*,5*R*)-5-Carboxymethyl Proline<sup>a</sup>

<sup>a</sup> (a) Ref 16. (b) PNB bromoacetate, CH<sub>3</sub>CN, 40 h. (c) Triphenylphosphine, triethylamine, CH<sub>2</sub>Cl<sub>2</sub>, 20 h. (d) Sodium cyanoborohydride, acetic acid, CH<sub>3</sub>CN. (e) Pd(OH)<sub>2</sub>/C, H<sub>2</sub>, EtOH. (f) Trifluoroacetic acid.

Scheme 4: Synthesis of (2*S*,5*S*)-5-Carboxyethyl Proline and 5-Oxo-hexahydropyrrolizine-3-carboxylic Acid<sup>a</sup>

<sup>a</sup> (a) Methyl diethylphosphonoacetate, potassium hydride, DMF, 1 h. (b) Lithium borohydride, diethyl ether, 3 h. (c) Carbon tetrabromide, triphenylphosphine, CH<sub>2</sub>Cl<sub>2</sub>, 20 min. (d) Sodium cyanide, DMSO, 3 h. (e) Sodium hydroxide, 30% hydrogen peroxide, MeOH/H<sub>2</sub>O, 18 h. (f) Trifluoroacetic acid (g) Δ Toluene, 5 d.

worked up under standard conditions. The two diastereomeric products were separated by repeated chromatography on silica gel using 5/95 ethyl acetate/hexane [3.86 g, 8.5 mmol, total yield 96%; separated yield (2*S*,5*S*) 965 mg, 2.1 mmol (24%); (2*S*,5*R*) 2.90 g, 6.4 mmol (72%)]. A degassed solution of the protected carboxymethyl proline (1.88 g, 4.14 mmol) in ethanol (100 mL) was hydrogenated at 55–60 psi over Pearlman's catalyst (300 mg, 15% loading). The *tert*-butyl ester (806 mg, 3.5 mmol) was removed with trifluoroacetic acid (15 mL). The crystalline (2*S*,5*R*)-CMPr was then triturated with acetone, filtered, and dried: 548 mg, 3.2 mmol, 77% yield (2 steps); mp 220 °C (dec); [α]<sub>D</sub><sup>25</sup> –60.0° (c = 1 H<sub>2</sub>O). <sup>1</sup>H NMR: δ 4.21 (dd, *J* = 4.8, 9.2 Hz, 1H), 3.97 (m, 1H), 2.92 (m, 2H), 2.34 (m, 1H), 2.22 (m, 2H), 1.74 (m, 1H); <sup>13</sup>C NMR: δ 174.6, 174.3, 61.3, 57.2, 36.1, 28.9, 28.2; IR: 3420, 2668, 1728, 1613, 1395; HRMS calcd for C<sub>7</sub>H<sub>11</sub>NO<sub>4</sub> [M+H<sup>+</sup>]: 174.0766, found 174.0760.

(D) *Synthesis of (2S,5S)-5-Carboxyethyl Proline (Scheme 4).* *N*-Boc-(2*S*,5*S*)-methoxycarbonylmethyl proline *tert*-butyl ester was prepared following a published protocol (15). Methyl diethyl phosphonoacetate (5.55 mL, 30.2 mmol) was added to 30% KH/mineral oil (4.05 g, 30.2 mmol) in 100 mL of dry DMF under an argon atmosphere. *N*-Boc-(2*S*)-5-hydroxy-proline *tert*-butyl ester (7.24 g, 25.2 mmol) in 50 mL of dry DMF was added and the mixture was stirred overnight. The solution was poured into 900 mL of sat. NH<sub>4</sub>Cl and extracted with diethyl ether (2 × 250 mL). After aqueous workup, *N*-Boc-(2*S*,5*S*)-methoxycarbonylmethyl proline *tert*-butyl ester was purified by silica gel chromatography (hexane) to yield a white solid, which was recrystallized from boiling hexane (6.74 g, 19.6 mmol, 78%



yield). The methyl ester (5.34 g, 15.6 mmol) in 90 mL of diethyl ether was reduced with  $\text{LiBH}_4$  (424 mg, 19.5 mmol) for 2 h at room temperature. *N*-Boc-(2*S*,5*S*)-2-hydroxyethyl proline *tert*-butyl ester was purified by silica gel chromatography (20/80 ethyl acetate/hexane) (4.71 g, 14.9 mmol, 96% yield). The alcohol (4.49 g, 14.3 mmol) was dissolved in 60 mL of  $\text{CH}_2\text{Cl}_2$  containing carbontetrabromide (5.91 g, 17.8 mmol) at 0 °C and treated with triphenylphosphine (5.61 g, 21.4 mmol). *N*-Boc-(2*S*,5*S*)-2-bromoethyl proline *tert*-butyl ester was purified by silica gel chromatography (10/90 ethyl acetate/hexane). The yellow solid obtained was recrystallized from boiling hexane (4.15 g, 11.0 mmol, 77% yield). The bromide (3.94 g, 10.4 mmol) was added to sodium cyanide (613 mg, 12.5 mmol) in DMSO and allowed to stir for 3 h. The mixture was poured into 400 mL of  $\text{dH}_2\text{O}$  and extracted into diethyl ether ( $2 \times 150$  mL) and *N*-Boc-(2*S*,5*S*)-2-cyanoethyl proline *tert*-butyl ester was purified by silica gel chromatography (20/80 ethyl acetate/hexane). The slightly yellow solid obtained was recrystallized from boiling hexane (3.11 g, 9.6 mmol, 92% yield). The nitrile (3.11 g, 9.6 mmol) was added to a mixture of 30 mL of methanol/20 mL of  $\text{dH}_2\text{O}$ /15 mL 30%  $\text{H}_2\text{O}_2$  containing sodium hydroxide (2.3 g, 57.6 mmol) and allowed to stir overnight. After alkaline and acidic workup, *N*-Boc-(2*S*,5*S*)-2-carboxyethyl proline *tert*-butyl ester was obtained as a white solid and recrystallized from boiling hexane (2.4 g, 7.0 mmol, 73% yield). The protected acid (1.0 g, 2.9 mmol) was treated with TFA. The crude crystalline product was triturated with ether, taken up in a minimal amount of  $\text{H}_2\text{O}$  ( $\sim 1$  mL), and precipitated by the addition of acetone (50 mL). CEP, contaminated with a small amount of the (2*S*,5*R*)-diastereomer, was obtained as a fine white powder: 420 mg, 2.2 mmol, 76% yield; mp 182–184 °C.  $^1\text{H}$  NMR:  $\delta$  4.15 (t,  $J = 8.4$  Hz, 1H), 3.72 (m, 1H), 2.51 (m, 2H), 2.45 (m, 1H), 2.22 (m, 1H), 2.09 (m, 1H), 1.99 (m, 2H), 1.75 (m, 1H);  $^{13}\text{C}$  NMR:  $\delta$  176.6, 173.7, 60.3, 59.7, 30.3, 29.5, 28.0, 26.1; IR: 2953, 1709, 1610, 1560, 1388, 1220  $\text{cm}^{-1}$ ; HRMS calcd for  $\text{C}_8\text{H}_{13}\text{NO}_4$  [ $\text{M}+\text{H}^+$ ]: 188.0917, found 188.0922.

**Syntheses of Alternate Products.** (A) *Synthesis of 5-Oxo-hexahydropyrrolizine-3-carboxylic Acid*. CEP (400 mg, 2.11 mmol), dissolved in 20 mL of  $\text{dH}_2\text{O}$ , was placed into a round-bottomed flask containing 200 mL of toluene equipped with a reflux condenser and a Dean–Stark apparatus. The solution was heated to reflux for 5 days with azeotropic removal of water. The mixture was cooled and concentrated in vacuo. A portion of the residue ( $\sim 60$  mg) was solubilized in 30 mL of 0.05% ammonium bicarbonate, and 1 mL portions were injected onto a Phenomenex Primesphere  $5\mu$  C18-MC 3 semi-prep column with 0.05% ammonium bicarbonate as the eluant. The fractions were collected and lyophilized to yield 32.5 mg (2*S*,5*S*) and 3.5 mg (2*S*,5*R*) in a diastereomeric ratio of 9.2:1, in accord with the literature for the initial coupling process (15): 36 mg, 0.21 mmol, 60% total yield; (major diastereomer) mp 98–100 °C;  $[\alpha]^{25}_{\text{D}} -159.2^\circ$  (c 1,  $\text{H}_2\text{O}$ ).  $^1\text{H}$  NMR:  $\delta$  4.12 (t(app),  $J = 8.0$  Hz, 2H), 2.83 (dt,  $J = 9.6$  Hz, 10.4 Hz, 1H), 2.6 (dt,  $J = 8.0$  Hz, 12.8 Hz, 1H), 2.45 (dd,  $J = 9.6$  Hz, 12.4, 1H), 2.31 (m, 1H), 2.06 (m, 1H), 1.99 (m, 1H), 1.80 (p(obs)  $J = 10.4$  Hz, 1H), 1.40 (p(obs),  $J = 10.4$  Hz, 1H);  $^{13}\text{C}$  NMR:  $\delta$  179.0, 176.5, 63.1, 56.4, 34.6, 32.8, 31.1, 25.7; IR: 2944, 1718, 1636, 1458, 1275  $\text{cm}^{-1}$ ; HRMS calcd for  $\text{C}_8\text{H}_{11}\text{NO}_3$  [ $\text{M}+\text{H}^+$ ]: 170.0812, found 170.0814.

(B) *Synthesis of (3*S*,5*S*)-Carbapenam-3-carboxylic Acid*. Carbapenam was synthesized from L-pyrroglutamic acid according to a published procedure (8): 0.4 mmol, 85% yield; mp 125 °C (dec);  $[\alpha]^{25}_{\text{D}} -148.0^\circ$  (c 1,  $\text{H}_2\text{O}$ ).  $^1\text{H}$  NMR:  $\delta$  4.17 (t,  $J = 8.4$  Hz, 1H), 3.83 (m, 1H), 3.22 (dd,  $J = 4.4$  Hz, 16.0 Hz, 1H), 2.66 (dd,  $J = 1.6$  Hz, 16.4 Hz, 1H), 2.59 (m, 1H), 2.18 (m, 1H), 2.05 (m, 1H), 1.48 (m, 1H);  $^{13}\text{C}$  NMR: 180.1, 179.2, 61.2, 52.9, 40.1, 35.9, 30.1; IR: 3430, 2927, 1742, 1615, 1400  $\text{cm}^{-1}$ ; ESI-MS calcd for  $\text{C}_7\text{H}_8\text{NO}_3$  [ $\text{M}-\text{H}^+$ ]: 154.1, found 154.2, MS/MS 112 (ketene).

**CarC Cell Free Extract.** *E. coli* BL21(DE3) cells transformed with pET24a/*carC* (8) were grown at 37 °C in 2 $\times$  YT medium supplemented with 50  $\mu\text{g}/\text{mL}$  kanamycin A. The cells were induced ( $\text{OD}_{600} = 0.65$ ) with 1 mM IPTG at 22 °C, harvested by centrifugation 3 h post-induction, and frozen as a pellet in liquid nitrogen. Four grams of cells were obtained from 1 L growth. The frozen cells resuspended in ice-cold lysis buffer (50 mM Tris HCl, pH 8.5, 20% glycerol, 10 mM KCl, 10  $\mu\text{M}$  EDTA, 1 mM benzamidine, 10 mM DTT) were lysed by incubating for 10 min at 4 °C with lysozyme (1 mg) under anaerobic conditions. Addition of Brij-58 to a final concentration of 0.1% (w/v) was followed after 10 min of stirring at 4 °C by the addition of DNase/RNase ( $\sim 1$  mg each). After removal of cell debris by centrifugation, the cell-free extract was stored at  $-80$  °C in 1 mL aliquots.

**Carbapenam Synthetase/CarC Coupled Bioassay.** The carbapenam synthetase/CarC coupled reaction included 1.0 mM ascorbate, 5 mM  $\alpha$ -ketoglutaric acid, 1.5 mM ATP– $\text{Mg}^{2+}$ , 1.5 mM CMPr, 4.5 mg/mL of carbapenam synthetase, and either 1 mL of CarC cell-free extract, or 1.6 mg/mL pure CarC. The control for the reaction components contained 1.0 mM ascorbate, 5 mM  $\alpha$ -ketoglutaric acid, 1.5 mM ATP– $\text{Mg}^{2+}$ , 1.5 mM CMPr, and 2 mM carbapenam, while a second control contained 4.5 mg/mL of carbapenam synthetase instead of the carbapenam. The control reaction for CarC activity contained 1.0 mM ascorbate, 5 mM  $\alpha$ -ketoglutaric acid, 2 mM carbapenam, and either 1 mL of CarC cell-free extract or 1.6 mg/mL pure CarC. The reactions were run in 20 mM KPi, pH 7.6. Two hundred microliters of the reaction mixture was spotted at different time points on a paper disk on an LB agar plate infused with *E. coli* SC 12155, a  $\beta$ -lactam supersensitive mutant strain (17). Following incubation of the plate at 28 °C for 18 h, (5*R*)-carbapen-2-em-3-carboxylic acid production was detected by visualization of antibiosis of *E. coli* SC 12155.

**Carbapenam Synthetase Assays.** PPI release catalyzed by carbapenam synthetase was detected using a modified coupled enzyme assay described by Van Pelt and Northrop (18). The enzymatic reaction was followed at 340 nm ( $\epsilon_{340} = 6.22 \text{ mM}^{-1} \text{ cm}^{-1}$ ) by the increase in the rate of production of NADPH. The reaction was performed at 22 °C in a buffer system of 80 mM piperazine and 100 mM HEPES (19), pH 7.8, 10 mM  $\text{MgCl}_2$ , 1 mM DTT with 0.2 mM UDP-glucose, 0.2 mM  $\beta$ NADP, and 0.2  $\mu\text{M}$  glucose-1,6-bisphosphate. The concentrations of the coupling enzymes used were 2 U/mL phosphoglucosmutase, 1 U/mL glucose-6-phosphate dehydrogenase, and 4 U/mL UDP-glucose pyrophosphorylase. Carbapenam synthetase activity was also assayed by coupling AMP production to the reactions of myokinase, pyruvate kinase, and lactate dehydrogenase (20). The enzymatic

reaction was followed at 340 nm by the increase in the rate of NADH consumption. The reaction was performed at 22 °C in the same buffer system described above, 10 mM MgCl<sub>2</sub>, 1 mM DTT with 1 mM phosphoenol pyruvate, and 0.2 mM NADH. The concentrations of the coupling enzymes used were 15–18 U/mL pyruvate kinase and lactate dehydrogenase, and 19 U/mL myokinase.

**Initial Velocity Studies.** The initial velocity patterns were measured with the PPi coupled enzyme assay described above. Initial velocity measurements were determined at various concentrations (0.075, 0.1, 0.15, 0.25, and 0.75 mM) of ATP in the presence of different fixed concentrations (0.075, 0.1, 0.15, 0.25, and 0.75 mM) of the CMPr. Assay reactions were run in triplicate.

**Product and Dead-End Inhibition Studies.** Inhibition experiments were carried out in a reaction mixture with one of the two substrates present at saturating concentration and with the concentration of the second substrate varied with several fixed levels of inhibitor. ATP and CMPr concentrations were respectively 0.7 and 1.5 mM when held constant. The concentrations of ATP and CMPr when varied were 0.1–0.75 mM for both. The concentrations of inhibitors when varied were 0–1 mM carbapenam, 0–1 mM AMP, 0–0.025 mM PPi, 0–80 mM L-proline, 0–50 mM for 5-aminovaleric acid, 6-aminocaproic acid, and L-aspartic acid. The PPi coupled enzyme assay was used for the inhibition studies in the presence of AMP and carbapenam. For PPi and proline inhibition studies, the AMP coupled enzyme assay described above was used.

**Determination of Steady-State Rate Constants for Alternate Substrates.** Initial velocities were measured using the PPi coupled enzyme assay at 0.75 mM ATP, unless otherwise noted. The rate of AMP formation was checked at one substrate concentration using the AMP coupled enzyme assay. The concentrations used in the assay were 0.75–9 mM (2*S*,5*R*)-CMPr, 1–20 mM (2*R*,5*R*)-CMPr, 0.25–8.66 mM CEP, 1–50 mM L-aminoadipic acid, 5–100 mM D-aminoadipic acid, 2–12 mM D,L-aminopimelic acid, 18.6–100 mM L-glutamic acid, 2–41.7 mM adipic acid, 2–12 mM pimelic acid, and 10–120 mM glutaric acid. Typically six different substrate concentrations were used in the assay.

**Steady-State Kinetic Analysis.** All data were fitted using the FORTRAN programs of Cleland (21). Initial velocity patterns were fitted to eqs 1 or 2. Competitive, uncompetitive, and noncompetitive inhibition patterns were fitted to eqs 3, 4, and 5, respectively.

$$v/[E_0] = k_{\text{cat}}A/[K_m + A] \quad (1)$$

$$v/[E_0] = k_{\text{cat}}AB/[K_aB + K_bA + AB + K_{ia}K_b] \quad (2)$$

$$v/[E_0] = k_{\text{cat}}A/[K_m(1 + I/K_{is}) + A] \quad (3)$$

$$v/[E_0] = k_{\text{cat}}A/[K_m + A(1 + I/K_{ii})] \quad (4)$$

$$v/[E_0] = k_{\text{cat}}A/[K_m(1 + I/K_{is}) + A(1 + I/K_{ii})] \quad (5)$$

**Investigation of the Reaction Catalyzed by Carbapenam Synthetase with Alternate Substrates by HPLC and ESI-MS.** Reactions were run at 22 °C in 100 mM KPi, pH 7.8, with 1 mM DTT and 10 mM ATP/Mg<sup>2+</sup>. The concentrations of the alternate substrates were 12 mM CEP, 20 mM L-

aminoadipic acid, and 50 mM L-glutamic acid. Carbapenam synthetase concentration was 1.25 mg/mL except in the reaction with L-glutamic acid where it was 1.6 mg/mL. A control reaction without enzyme was performed in parallel. Aliquots of the reaction were removed at different times and heated at 100 °C for 1 min. After the precipitated enzyme was removed by centrifugation, the aliquots were analyzed by HPLC using an analytical Phenomenex Prodigy column (4.6 × 250 mm) at 210 nm with 100 mM KPi, pH 7.8, as the elution buffer. At 1 mL/min, PPi, L-aminoadipic acid and L-glutamic acid elute at 2.7 min, CEP at 3.6 min, pyroglutamic acid at 3.7 min, 6-oxo-piperidine-2-carboxylic acid at 6.0 min, ATP and AMP as a broad peak around 9 min, and 5-oxo-hexahydropyrrolizine-3-carboxylic acid at 27 min. The internal standard used for the HPLC analysis was 2 mM 6-oxo-piperidine-2-carboxylic acid, except in the reaction with L-aminoadipic acid in which 2 mM pyroglutamic acid was used. The HPLC traces have all been normalized to the internal standard peak height. The peak coeluting with synthetic 5-oxo-hexahydropyrrolizine-3-carboxylic acid was collected from multiple injections, concentrated, and desalted by injecting on the same analytical HPLC column. 5-Oxo-hexahydropyrrolizine-3-carboxylic acid elutes with dH<sub>2</sub>O as a broad peak at ~22 min. The identity of the  $\gamma$ -lactam product was further confirmed by ESI-MS: *m/z* 168.5 (M–H). ESI spectrum was acquired in negative ion mode on a Finnigan LCQ ion trap mass spectrometer with an ESI source. The capillary temperature was kept at 225 °C. The samples were prepared in 1:1 dH<sub>2</sub>O/ acetonitrile with 1% NH<sub>4</sub>OH prior to direct injection into the ESI chamber using a syringe pump at a flow rate of 25  $\mu$ L/min. Typically 30 scans were averaged for each spectrum.

**Carbapenam Synthetase Catalyzed Reaction of CMPr in the Presence of Hydroxylamine.** Reactions were run at 22 °C in 100 mM KPi, pH 7.8, with 1.5 mM ATP/Mg<sup>2+</sup>, 1.5 mM CMPr, 1 mM DTT, and 100 mM hydroxylamine-HCl. The concentration of carbapenam synthetase was 0.55 mg/mL. Two control reactions without carbapenam synthetase or CMPr were also run. Aliquots of 80  $\mu$ L were withdrawn at different times and quenched by addition of 10  $\mu$ L of 5% TFA and 10  $\mu$ L of 10% FeCl<sub>3</sub>·6H<sub>2</sub>O in 2 N HCl. After removal of the precipitated protein by centrifugation, an absorbance scan in the visible region of the reaction mixture was taken to detect the colored complex of the hydroxamate derivative with ferric chloride (22).

**Carbapenam Synthetase Catalyzed Reactions of Diacids in the Presence of Hydroxylamine.** (A) *Adipic Acid.* Formation of AMP was detected in the reaction catalyzed by carbapenam synthetase in 250 mM MOPS, pH 7.2, with 1 mM DTT, 0.75 mM ATP, 40 mM adipic acid, and hydroxylamine using the AMP coupled enzyme assay described above. The stock solution of hydroxylamine was titrated to pH 7.2 and added to the reaction mixture to a final concentration of 100 or 40 mM. To test whether AMP formation was dependent only on the reaction of carbapenam synthetase with adipic acid and ATP in the presence of hydroxylamine, similar reactions were performed in the absence of adipic acid (no formation of AMP was observed) and in the absence of carbapenam synthetase (no formation of AMP was observed). The effect of hydroxylamine on carbapenam synthetase activity was tested by monitoring PPi production in the reaction mixture described above with or

without hydroxylamine (no effect was observed). The formation of the hydroxamate derivative in the reaction catalyzed by carbapenam synthetase in 250 mM MOPS, pH 7.2, with 1 mM DTT, 1.5 mM ATP, 40 mM adipic acid, and 100 mM hydroxylamine was confirmed by the ferric chloride assay as described above. Control reactions were run in the absence of adipic acid (no formation of the hydroxamate derivative was observed) and in the absence of carbapenam synthetase (no formation of the hydroxamate derivative was observed) to test whether hydroxamate formation was dependent only on the reaction of carbapenam synthetase with adipic acid and ATP.

(B) *Glutaric Acid*. AMP release was compared in the reaction catalyzed by carbapenam synthetase with 100 mM glutaric acid and in the presence and absence of 100 mM hydroxylamine. The AMP coupled enzyme assay was performed as described in the reaction with adipic acid.

*ATP-Pi Isotope Exchange Studies*. Reactions were run in a buffer system of 80 mM piperazine and 100 mM HEPES, pH 7.8, with 4 mM ATP, 4 mM CMPr, 1 mM DTT, 10 mM MgCl<sub>2</sub>, and 0.1 mM PPi with 0.3  $\mu$ Ci of [<sup>32</sup>P]PPi (4 Ci/mmol). Reactions were started by addition of carbapenam synthetase (0.017–0.070 nmol) in the presence of 0.1 mg/mL BSA. Two control reactions were run one without CMPr and one without carbapenam synthetase. After 1 and 2 h at 22 °C, the reactions were quenched and analyzed following a published protocol (23).

## RESULTS

*Syntheses of Alternate Substrates*. Synthesis of CMPr favoring the (2*S*,5*S*) stereochemistry was accomplished by the coupling method of Pedregal et al. to make protected carboxymethyl prolines (15). Utilizing *tert*-butyl esters as carboxyl protecting groups in this system, they produced (2*S*,5*S*)-CMPr/(2*S*,5*R*)-CMPr in a ratio of 17:1. This high degree of diastereoselectivity observed by Pedregal was determined by <sup>1</sup>H NMR analysis of the deprotected CMPr. In our hands, this method yielded a diastereomeric ratio of  $\geq$ 19:1. The method of Rapoport (16) was used to favor establishment of the (5*R*) configuration in CMPr. This protocol requires a greater number of steps than that used for the synthesis of the (2*S*,5*S*)-diastereoisomer and a lengthy separation of diastereomers by silica gel chromatography. The (2*S*) configuration of the vinylogous amide intermediate, set from L-glutamate, directs hydrogenation/hydride reduction to the less hindered face of the molecule to yield the (5*R*) stereoisomer predominantly. Hydride reduction yielded (2*S*,5*R*)-CMPr/(2*S*,5*S*)-CMPr in a 3:1 ratio, which were separated by silica gel chromatography to give (2*S*,5*R*)-CMPr free of the (2*S*,5*S*) diastereomer by TLC and <sup>1</sup>H NMR analysis.

*Characterization and Functional Assignment of Carbapenam Synthetase*. Soluble and active *E. carotovora* carbapenam synthetase was obtained from overexpression of the plasmid pET24a/*carA* transformed in *E. coli* BL21(DE3) cells. Carbapenam synthetase was purified to homogeneity as judged by SDS-PAGE gel electrophoresis using a protocol involving ammonium sulfate precipitation, anion exchange, and gel filtration chromatography. A typical yield is 4.9 mg of pure enzyme/g of wet cell paste. Carbapenam synthetase and molecular weight standards were subjected

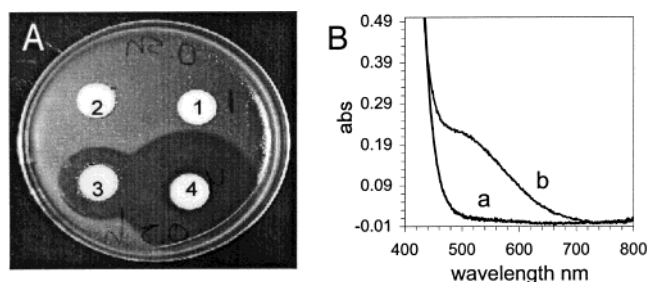


FIGURE 1: (A) Carbapenam synthetase/CarC coupled bioassay. (5*R*)-Carbapen-2-em-3-carboxylic acid production was visualized by antibiosis on a lawn of the  $\beta$ -lactam supersensitive *E. coli* strain SC 12155. All four reactions shown contained 5 mM  $\alpha$ -ketoglutarate and 1 mM ascorbate in 20 mM KPi, pH 7.6, and were spotted on each disc after 30 min at 22 °C. Reaction 1 also contained 1.5 mM ATP/Mg<sup>2+</sup>, 1.5 mM CMPr, and 2 mM carbapenam. Reaction 2 was run in the presence of 1.5 mM ATP/Mg<sup>2+</sup>, 1.5 mM CMPr, and 4.5 mg/mL of carbapenam synthetase. Reaction 3 was performed as reaction 2 with the addition of 1.6 mg/mL of pure CarC. Reaction 4 contained 2 mM carbapenam and 1.6 mg/mL of pure CarC. (B) Carbapenam formation detected by the hydroxylamine/FeCl<sub>3</sub> colorimetric assay. All reactions were run in the HEPES/piperazine buffer system, pH 7.8, with 1.5 mM ATP/Mg<sup>2+</sup>, 1 mM DTT, and 100 mM hydroxylamine-HCl. Spectra (a) are control reactions in the absence of either carbapenam synthetase or CMPr. Spectrum (b) is a 4 h aliquot of the reaction with 0.55 mg/mL carbapenam synthetase and 1.5 mM CMPr.

to discontinuous native electrophoresis at five different concentrations of acrylamide. The Ferguson plot (24) generated with the molecular weight standards was used to estimate the molecular mass of native carbapenam synthetase as 119 kDa (calcd for monomer 56 kDa), indicating that the native enzyme exists as a homodimer (one band is observed under denaturing conditions, Supporting Information).

The CMPr-dependent hydrolysis of ATP to AMP and PPi for the reaction catalyzed by carbapenam synthetase was observed by coupled enzyme assays. Comparable initial linear rates of formation of AMP and PPi were measured using both assays. Direct observation by HPLC chromatography of the probable product, carbapenam, was hampered by a very low extinction coefficient and by Mg<sup>2+</sup> catalyzed hydrolysis of the carbapenam to CMPr (25, 26, unpublished results). Attempts were made to minimize the Mg<sup>2+</sup> catalyzed hydrolysis by running the reaction with 0.5 equiv of Mg<sup>2+</sup> in the presence of 1 equiv of ATP. Detection by ESI-MS failed since it was found that the presence of Mg<sup>2+</sup> quenched the parent peak of a synthetic standard of carbapenam.

A carbapenam synthetase/CarC coupled bioassay was used to show that the product of the carbapenam synthetase reaction is a substrate for CarC. Both the synthetically obtained carbapenam and the product of the reaction of carbapenam synthetase with CMPr and ATP/Mg<sup>2+</sup> gave negative results in the bioassay with the  $\beta$ -lactam antibiotic supersensitive *E. coli* strain SC 12155 (Figure 1A, reactions 1 and 2). However, antibiosis of the *E. coli* cells occurred when the carbapenam synthetase was coupled with CarC (Figure 1A, reaction 3). Similar results were obtained when a cell-free extract of CarC was used. CarC, the last enzyme of the pathway, carries out an isomerization-desaturation reaction on the carbapenam in the presence of  $\alpha$ -KG and ascorbate to produce the antibiotic (5*R*)-carbapen-2-em-3-carboxylic acid, as shown in reaction 4 of Figure 1A where chemically synthesized carbapenam was used as a substrate for CarC (8, 9). Additional evidence for the formation of



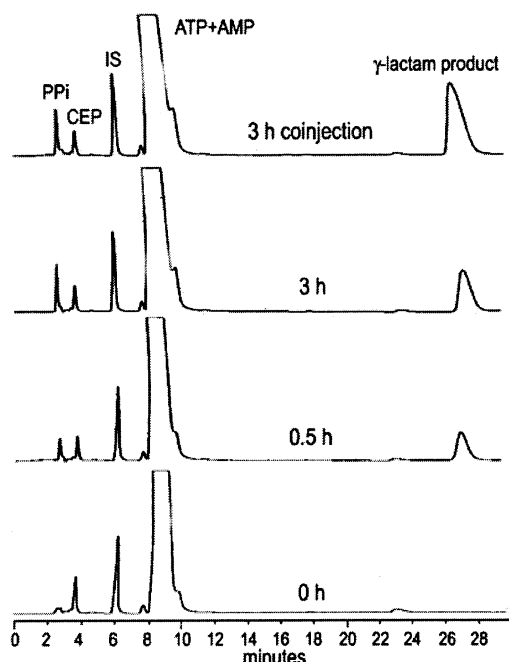


FIGURE 2: Reverse phase HPLC analysis of the reaction catalyzed by carbapenam synthetase in 100 mM KPi, pH 7.8, with 1 mM DTT, 10 mM ATP/Mg<sup>2+</sup> and 12 mM CEP; detection at 210 nm. The internal standard used for the HPLC analysis was 6-oxo-piperidine-2-carboxylic acid (IS).

the  $\beta$ -lactam ring catalyzed by carbapenam synthetase is provided by the appearance of an absorption peak at  $\sim 495$  nm typical of the colored complex formed by the hydroxamate derivative (5-hydroxycarbamoylmethyl-pyrrolidine-2-carboxylic acid) with ferric chloride (Figure 1B, spectrum b). The hydroxamate derivative of the carbapenam was obtained by running the enzyme reaction in the presence of hydroxylamine. Under the mild conditions of the experiment, hydroxylamine will react with acid anhydrides, acid chlorides, thiol esters, acyl phosphate, and *N*-acyl imidazoles but not with esters, aldehydes, amides, and ketones (27). The ability of hydroxylamine to act as a nucleophile at pH 7.8 causing ring opening of the  $\beta$ -lactam ring of carbapenam to form 5-hydroxycarbamoylmethyl-pyrrolidine-2-carboxylic acid was tested using synthetically prepared carbapenam. The reaction of hydroxylamine with the  $\beta$ -lactam bond occurs around neutral pH owing to the strained nature of this bicyclic ring system. Although 5-hydroxycarbamoylmethyl-pyrrolidine-2-carboxylic acid could also be formed from the reaction of hydroxylamine with the postulated acyladenylate intermediate, it is unlikely that this latter reaction contributes significantly to the accumulation of the hydroxamate derivative since the reaction was run under steady-state conditions where comparable rates of formation of AMP and PPI were observed. None of the components of the carbapenam synthetase reaction, including CMPr, interfere with the formation of the hydroxamate derivative (Figure 1B, spectra a).

To further prove the ability of carbapenam synthetase to catalyze an ATP dependent intramolecular amide bond formation the reaction with the alternate substrate, CEP was analyzed by reverse phase HPLC taking advantage of the increased stability of the postulated  $\gamma$ -lactam bicyclic product. In Figure 2 a peak increasing with time and coeluting with synthetic standard 5-oxo-hexahydropyrrolizine-3-carboxylic

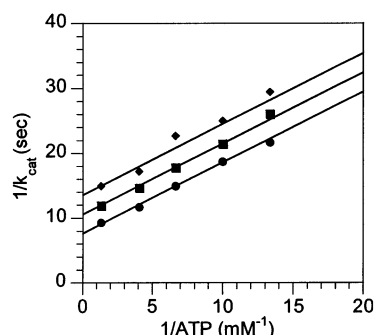


FIGURE 3: Dead-end inhibition by L-proline of the reaction catalyzed by carbapenam synthetase with 1.5 mM CMPr and ATP as the variable substrate. The concentrations of L-proline used from bottom to top were 0, 80, and 160 mM. The lines are the best fit of the data using eq 4.

acid is observed at  $\sim 27$  min. The CEP peak does not decrease significantly with time due to the particularly low extinction coefficient of the substrate, while PPI release can be observed in the increase of the peak at 2.7 min qualitatively in parallel with  $\gamma$ -lactam production. The identity of the peak at 27 min as 5-oxo-hexahydropyrrolizine-3-carboxylic acid was further confirmed by ESI-MS [calcd 168.2 (M-H), found 168.5 (M-H)] and MS<sup>n</sup> experiments.

**Steady-State Kinetic Studies.** The kinetic mechanism of *E. carotovora* carbapenam synthetase was determined by initial velocity, product inhibition, and dead-end inhibition studies using the AMP and PPI coupled enzyme assays described above. Double-reciprocal plots of initial velocity were obtained by varying ATP at different fixed levels of CMPr. The intersecting pattern observed (Supporting Information) is indicative of a sequential mechanism where all substrates must be bound to the enzyme before any product is released. Steady-state kinetic constants determined by fitting the data to eq 2 are shown in the first two rows of Table 1. The dissociation constants for ATP ( $K_{ia}$ ) and CMPr ( $K_{ib}$ ) were respectively  $0.31 \pm 0.06$  and  $0.63 \pm 0.18$  mM, greater than the corresponding  $K_m$  values.

To distinguish between an ordered and a random mechanism, product and dead-end inhibition studies were carried out at various concentrations of one substrate at a fixed saturating level of the second substrate in the presence of different concentrations or in the absence of the inhibitor (Table 2). The uncompetitive nature of the inhibition of the dead-end inhibitor, L-proline, versus ATP (Figure 3) is consistent with a mechanism with ordered substrate binding where ATP binds first followed by CMPr. The competitive inhibition exhibited by PPI versus ATP (Figure 4) allows the assignment of PPI as the last product released. AMP departure is surrounded by irreversible product release steps as indicated by the uncompetitive inhibition shown by AMP versus both substrates (Figure 5). The observed pattern of inhibition of carbapenam versus CMPr differs from the predicted patterns of a typical ordered Bi-Ter mechanism such as the one determined for the reversible reaction catalyzed by pigeon liver malic enzyme (28). Synthesized batches of carbapenam are contaminated by an impurity of the hydrolyzed compound, CMPr (9). The material used in the inhibition experiments contained 11% of CMPr as judged by <sup>1</sup>H NMR. When ATP is varied and CMPr is kept at a concentration six times its  $K_m$ , the impurity of CMPr in the inhibitor has no effect on the carbapenam inhibition pattern.

Table 1: Steady State Kinetic Parameters for Carbapenam Synthetase Measured at 22 °C and pH 7.8<sup>a</sup>

substrate	$K_m$ (mM)	$+\Delta^b$	$k_{cat}$ (s <sup>-1</sup> )	$-\Delta^c$	$k_{cat}/K_m$ (mM <sup>-1</sup> s <sup>-1</sup> )	$-\Delta^c$
ATP <sup>d</sup>	0.11 ± 0.02		0.28 ± 0.02		2.5 ± 0.4	
(2 <i>S</i> ,5 <i>S</i> )-CMP <sup>d</sup>	0.23 ± 0.04	1	0.28 ± 0.02	1	1.2 ± 0.1	1
(2 <i>S</i> ,5 <i>R</i> )-CMP <sup>r</sup>	7 ± 1	30	0.20 ± 0.03	1.4	0.027 ± 0.003	44
(2 <i>R</i> ,5 <i>R</i> )-CMP <sup>r</sup>	4.6 ± 0.3	20	0.122 ± 0.002	2.3	0.026 ± 0.001	46
CEP	3.4 ± 0.4	15	0.46 ± 0.02	0.6	0.13 ± 0.01	9
D,L-aminopimelic acid	9 ± 2	39	0.037 ± 0.004	7.6	0.0042 ± 0.0005	286
L-aminoadipic acid	17 ± 2	74	0.19 ± 0.01	1.5	0.011 ± 0.001	91
D-aminoadipic acid	32 ± 2	139	0.20 ± 0.01	1.4	0.0063 ± 0.0007	190
L-glutamic acid	29 ± 6	126	0.028 ± 0.001	10	0.0010 ± 0.0001	1200
pimelic acid <sup>e</sup>	6 ± 1	26	0.033 ± 0.004	8.5	0.006 ± 0.001	200
adipic acid <sup>e</sup>	20 ± 4	87	0.082 ± 0.007	3.4	0.0040 ± 0.0004	300
glutaric acid <sup>e</sup>	27 ± 2	117	0.040 ± 0.003	7	0.0015 ± 0.0003	800

<sup>a</sup> The kinetic parameters were determined by fitting the data to eq 1 unless otherwise noted. Reactions were performed as described under Experimental Procedures. <sup>b</sup> “ $+\Delta$ ” refers to the fold change above the  $K_m$  listed for the reaction with CMP<sup>r</sup>. <sup>c</sup> “ $-\Delta$ ” refers to the fold change below the  $k_{cat}$  or  $k_{cat}/K_m$  listed for the reaction with CMP<sup>r</sup>. <sup>d</sup> These kinetic parameters were determined by fitting the data to eq 2. <sup>e</sup> See Results.

Table 2: Product and Dead-End Inhibition of Carbapenam Synthetase<sup>a</sup>

inhibitor	variable substrate	$K_{is}$ (mM)	$K_{ii}$ (mM)	obsd pattern <sup>b</sup>	predicted pattern <sup>b,c</sup>
AMP	ATP		0.17 ± 0.02	UC	UC
AMP	CMP <sup>r</sup>		0.28 ± 0.01	UC	UC
PPi	ATP	0.012 ± 0.001		C	C
PPi	CMP <sup>r</sup>	0.005 ± 0.001	0.019 ± 0.007	NC	NC
carbapenam	CMP <sup>r</sup>		1.3 ± 0.1	UC	NC
carbapenam	ATP	1.3 ± 0.2	1.1 ± 0.1	NC	NC
l-proline	ATP		207 ± 12	UC	UC
l-proline	CMP <sup>r</sup>	90 ± 19		C	C

<sup>a</sup> The enzyme activity was measured in 10 mM MgCl<sub>2</sub>, 1 mM DTT, 80 mM piperazine, and 100 mM HEPES buffer system, pH 7.8, at 22 °C. When kept fixed, the concentration of ATP was 0.7 mM; that of CMP<sup>r</sup> was 1.5 mM. The kinetic parameters were determined by fitting the data to eqs 3, 4, or 5. <sup>b</sup> C, competitive inhibition; NC, noncompetitive inhibition; UC, uncompetitive inhibition. <sup>c</sup> Predicted pattern for an ordered Bi-Ter mechanism.

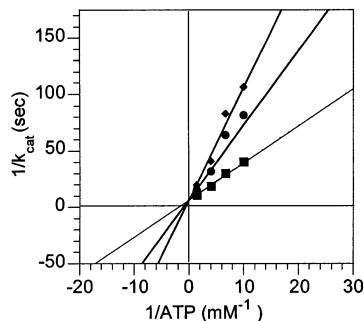


FIGURE 4: Product inhibition by PPi of the reaction catalyzed by carbapenam synthetase with 1.5 mM CMP<sup>r</sup> and ATP as the variable substrate. The concentrations of PPi used from bottom to top were 0, 0.0125, and 0.025 mM. The lines are the best fit of the data using eq 3.

When CMP<sup>r</sup> is the variable substrate, the presence of this impurity will diminish the slope of the inhibited plots. Eventually at low enough concentrations of CMP<sup>r</sup> the slope of the inhibited plots will tend to zero until they will cross the uninhibited plot. The presence of the contaminant in the carbapenam solution could account for the apparent uncompetitive inhibition pattern. In sum, these patterns would then be consistent with an ordered Bi-Ter mechanism where carbapenam is the first product released and AMP is the second. The absence of curvature in the carbapenam versus CMP<sup>r</sup> pattern at low concentration of varied substrate leads to a second more likely explanation. If the reaction is not reversible enough for the first product to show a slope effect as shown by the lack of <sup>32</sup>PPi/ATP exchange, then the carbapenam and the AMP releases are surrounded by irreversible steps as revealed by the uncompetitive nature

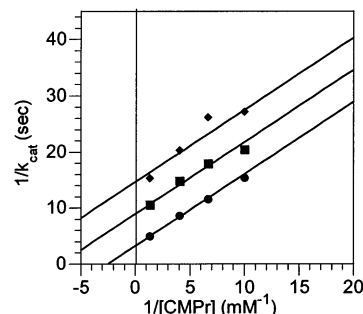


FIGURE 5: Product inhibition by AMP of the reaction catalyzed by carbapenam synthetase with 0.7 mM ATP and CMP<sup>r</sup> as the variable substrate. The concentrations of AMP used from bottom to top were 0, 0.5, and 1 mM. The lines are the best fit of the data using eq 4.

of the inhibition patterns. The noncompetitive pattern of carbapenam versus ATP would come from dead-end combination in the ATP site. In this case, the inhibition patterns are consistent with either a random or an ordered release of carbapenam and AMP.

*Carbapenam Synthetase Reaction with Alternative Amino Acids: Determination of the Steady-State Kinetic Parameters and HPLC Characterization of the Products.* To probe the substrate specificity and to gain insight into the substrate-binding site in the absence of a crystal structure, a number of alternate amino acids shown in Scheme 6 have been tested as potential substrates of carbapenam synthetase. The steady-state kinetic parameters for stereochemical and conformational CMP<sup>r</sup> analogues are shown in Table 1. Changes in the stereochemistry at C-2 or at both C-5 and C-2 have essentially no effect on  $k_{cat}$  values while they cause a 20- to



30-fold increase in  $K_m$  values. The presence of an additional methylene group in the side chain of CEP increases the  $K_m$  value by more than an order of magnitude. Interestingly, the carbapenam synthetase reaction with CEP, which retains the right stereochemistry at C-2 and C-5 but yields a 5,5-fused azobicyclic product (Figure 2) instead of a 4,5-fused product, is 1.6-fold faster than the reaction with CMPr.

To test the ability of carbapenam synthetase to catalyze intramolecular amide bond formation with acyclic amino diacids to form five-, six-, and seven-membered monocyclic products, the reaction was run with L-glutamic acid, D,L-aminopimelic acid, L- and D-aminoadipic acid. The nature of the products with these alternate substrates was confirmed by HPLC analysis with synthetic standards (Supporting Information). The reactions were studied by coupled enzyme assays and the kinetic parameters are shown in Table 1. The monotonic increase of the  $K_m$  values with each removal of a methylene group reflects the departure from four carbons between C-3 and C-7 in CMPr that is also retained in aminopimelic acid. When only one methylene group is left, such as in aspartic acid, the affinity with the active site of the enzyme is greatly diminished as shown by the both lack of catalysis, and the absence of inhibition by L-aspartic acid at a concentration as high as 50 mM. As already observed with the stereochemical analogues of CMPr, a change in stereochemistry from L- to D-aminoadipic acid has no effect on the  $k_{cat}$  value, but causes a 2-fold increase in  $K_m$ .

When compounds such as aminovaleric and aminocaproic acids, which are analogues lacking the  $\alpha$ -carboxylic group, respectively, of aminoadipic and aminopimelic acids, were tested as substrates for carbapenam synthetase, no catalysis was observed at concentrations as high as 50 mM. To determine whether the absence of catalysis is due to poor substrate recognition, an inhibition study was performed. Both aminovaleric and aminocaproic acids are very weak competitive inhibitors versus CMPr with  $K_{is} = 142 \pm 28$  mM and  $K_{is} = 168 \pm 48$  mM, respectively. The extremely high inhibition constants measured are consistent with catalysis hampered by poor binding affinity with the active site. Nonproductive binding might also contribute to the lack of observed catalysis. Removal of the other carboxylate in CMPr, the C-7 carboxylate, has less impact on binding affinity as illustrated by the lower  $K_{is}$  of L-proline versus CMPr (Table 2). The weak inhibitory effect of L-proline is not only the result of the removal of the C-7 carboxylate but also of the C-6 methylene group.

To test the role of the methylene group at C-3 and C-4 in CMPr in affinity to carbapenam synthetase, the reaction with 3-(carboxymethylamino)-propionic acid was studied. Looking at the CMPr molecule, a 3-(carboxymethylamino)-propionic acid moiety is visible from C-2 through N to C-5 and C-7, while an aminopimelic moiety is visible going from C-2 through C-3 to C-5 and C-7. Although aminopimelic acid is a substrate for the enzyme, no catalysis was observed with 3-(carboxymethylamino)-propionic acid at concentrations as high as 50 mM.

**Carbapenam Synthetase Reaction with Diacids.** A time delay of few minutes appears when AMP formation is detected in the reaction of carbapenam synthetase with glutaric acid (Supporting Information). Addition of 100 mM hydroxylamine to the reaction mixture causes disappearance of the delay (data not shown). In the carbapenam reaction

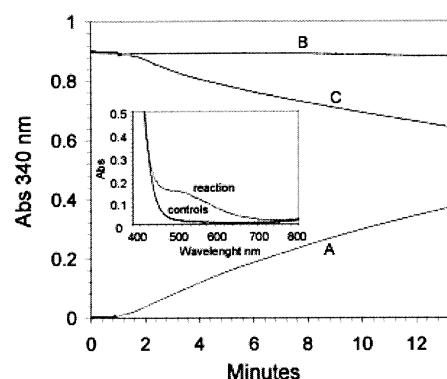


FIGURE 6: Detection of PPI (A) and AMP (B) production in the reaction catalyzed by carbapenam synthetase in 250 mM MOPS, pH 7.2, with 1 mM DTT, 0.75 mM ATP/Mg<sup>2+</sup> and 40 mM adipic acid. (C) Monitoring of AMP formation in the reaction described above in the presence of 100 mM hydroxylamine. Insets: FeCl<sub>3</sub> colorimetric assay of the reaction catalyzed by carbapenam synthetase in 250 mM MOPS, pH 7.2, with 1 mM DTT, 1.5 mM ATP/Mg<sup>2+</sup>, 40 mM adipic acid, and 100 mM hydroxylamine. Control reactions were run in the absence of either carbapenam synthetase or adipic acid.

with adipic and pimelic acid, only PPI release is observed and AMP formation occurs only if hydroxylamine is added to the reaction mixture (Figure 6). At neutral pH, hydroxylamine is a strong enough nucleophile to attack the carbonyl group of acyl-AMP compounds yielding AMP and a hydroxamate derivative (29, 30). Formation of this derivative was confirmed in the carbapenam synthetase reaction with adipic acid by the appearance of an absorption peak around 495 nm typical of the colored complex formed by the hydroxamate derivative with ferric chloride (Figure 6: insets). Taken together, these results suggest that the carbapenam synthetase reaction proceeds only up to the distal acyl-AMP diacid product. Favorable spontaneous formation of the six-membered glutaric anhydride in solution can account for the observed AMP release in the absence of hydroxylamine. The time lag observed indicates that formation of the glutaryl-adenylate compound is faster than the nonenzymic cyclization step. On the contrary, the adipoyl- and pimeloyl-adenylates are stable in solution as indicated by the absence of AMP release. This increased stability is likely due to less favorable cyclization reactions that would generate seven- and eight-membered ring anhydrides. In keeping with the order of product release, the appearance of PPI in the absence of hydroxylamine supports the view that all these distal acyl-AMP diacids are released into solution.

The steady-state rate constants for the carbapenam synthetase reactions with diacids were determined using the PPI coupled enzyme assay and are given in Table 1. Since the carbapenam synthetase reaction with the diacids stops at the formation of the acyl-adenylate intermediate, the comparison of these values with the parameters, especially  $k_{cat}$ , measured for CMPr and the amino diacids is not as unequivocal. The  $K_m$  values determined are similar to those measured for the corresponding amino diacids, suggesting that the removal of the amino group has little effect on substrate affinity.

## DISCUSSION

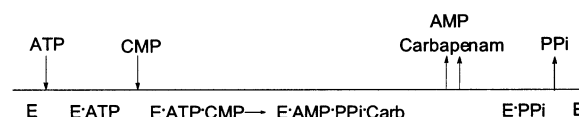
The main goal of this study is to investigate the reaction catalyzed by carbapenam synthetase. Specifically, we wanted to functionally, kinetically, and mechanistically characterize

the carbapenam synthetase reaction, and to elucidate the importance of structural elements on CMP<sub>r</sub> binding. Carbapenam synthetase shows sequence homology with both  $\beta$ -LS (22% identity, 36% similarity) and AS-B (17% identity, 31% similarity). All three catalyzed reactions are believed to proceed by activating a carboxyl group of the substrate through formation of a distal acyl-AMP amino diacid intermediate (Scheme 7). AS-B has two domains, an N-terminal domain where the hydrolysis of glutamine to glutamate and ammonia occurs, and a C-terminal domain where nucleophilic attack by the ammonia causes breakdown of  $\beta$ -aspartyl-AMP, formed from ATP and aspartate (31). In the  $\beta$ -LS structure, there is a common fold with AS-B (32). While the N-terminal domain of  $\beta$ -LS lacks the critical Cys residue necessary for glutaminase activity and is less organized, the C-terminal domain, the only catalytic domain, resembles that of AS-B. The chemical and structural similarities between these two enzymes have been interpreted as indications of an evolutionary link between  $\beta$ -LS and AS-B (23, 32). In this evolutionary process, the structural and catalytic machinery of AS-B for ATP binding and for synthesis of a distal acyl-AMP amino diacid intermediate was conserved, while the second binding site in the C-terminal domain has adapted to both bind a different substrate, and to promote the intramolecular cyclization reaction (32, 33). Sequence alignments of  $\beta$ -LS and AS-B with carbapenam synthetase show that, as in  $\beta$ -LS, the important N-terminal Cys residue is absent. The ATP binding site and several regions in the C-terminal domain are well-conserved between  $\beta$ -LS and carbapenam synthetase (34), indicating that the latter may be structurally related to  $\beta$ -LS and, therefore, to AS-B.

The isolation of CMP<sub>r</sub> and carbapenam from the fermentation medium of *E. coli* cells transformed, respectively, with pET24a/*carB* and with pET24a/*carAB* provided a strong indication of the potential substrate and product of the carbapenam synthetase reaction (8). We proceeded, therefore, to characterize in vitro the carbapenam synthetase reaction. AMP and PPi formation was dependent upon the addition of CMP<sub>r</sub> to the reaction mixture, as expected if the intramolecular amide bond formation of CMP<sub>r</sub> were coupled to ATP hydrolysis. Attempts to identify the nature of the product by HPLC or ESI-MS failed owing to the low extinction coefficient and to the instability of the  $\beta$ -lactam ring of the carbapenam in the presence MgCl<sub>2</sub>. Evidence for the catalysis of  $\beta$ -lactam ring formation by carbapenam synthetase was provided by formation of a hydroxamate derivative when the reaction was run in the presence of hydroxylamine, and by the ability of the enzyme to synthesize from CMP<sub>r</sub> and ATP a compound in vitro which is the substrate for CarC. The formation and characterization of the stable 5,5-fused azobicyclic product upon reaction with CEP as substrate established that an ATP-dependent intramolecular amide bond formation is catalyzed by carbapenam synthetase. On the basis of these findings, carbapenam synthetase catalyzes the synthesis of the carbapenam from CMP<sub>r</sub> with concomitant hydrolysis of ATP to AMP and PPi.

Initial velocity, product, and dead-inhibition studies for carbapenam synthetase were in agreement with an ordered addition of substrates (Scheme 5) in which ATP binds first followed by CMP<sub>r</sub> and with PPi as the last product released. The product inhibition patterns of carbapenam and AMP

Scheme 5

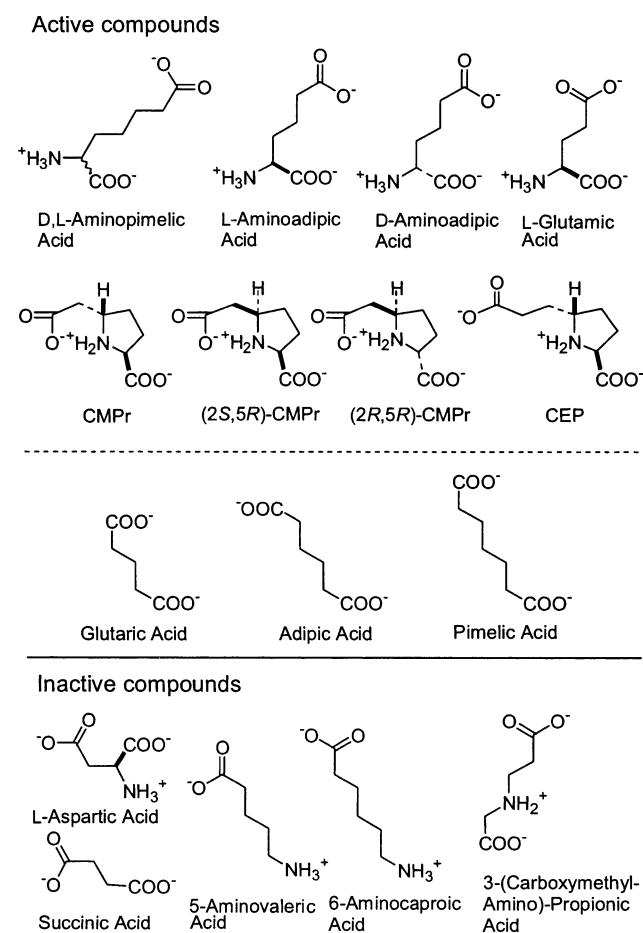


could not distinguish between a random or ordered release of these products. Ordered addition of substrates with ATP binding first was also reported for  $\beta$ -LS (23) and AS-B (35). The absence of AMP inhibition patterns in the  $\beta$ -LS reaction prevented a complete assignment of the order of the first two products, AMP and deoxyguanidinoproclavaminic acid, but also in this reaction PPi is the last product released (23). The crystal structures of  $\beta$ -LS with all products and with intermediates bound provide a structural explanation for the release of PPi as the last product. The PPi binding site in both of these structures is situated deep in the active site cleft protected from solvent by the other products and intermediates and by a loop comprising residues 444–453 (33). For PPi to be released, the active site must open and the other two products likely must diffuse out first.

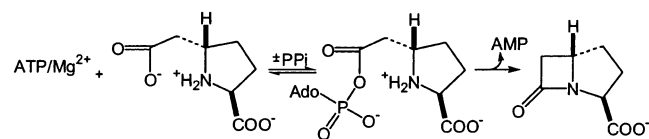
The first step in the reaction of both AS-B and  $\beta$ -LS is the activation of a carboxyl group in the substrate through the synthesis of a distal acyl-AMP amino diacid intermediate. Evidence for an acyladenylate intermediate is usually provided by either a <sup>32</sup>PPi exchange experiment into ATP, or by transfer of <sup>18</sup>O label from the carboxylate of the substrate to AMP (36). Evidence of the  $\beta$ -aspartyl-AMP intermediate was provided in the AS-B reaction by observing <sup>18</sup>O transfer from aspartate to AMP (35). Interestingly, an acyladenylate intermediate in the  $\beta$ -LS reaction was trapped in crystals of  $\beta$ -LS that were soaked with ATP and *N*<sup>2</sup>-(carboxymethyl)-L-arginine, a truncated substrate analogue and dead-end inhibitor (35). As previously observed in the asparagine synthetase (35) and in the  $\beta$ -LS reactions (23), no <sup>32</sup>PPi/ATP exchange was seen in the carbapenam synthetase reaction. The absence of PPi exchange suggests that distal acyl-AMP amino diacid formation is irreversible, although acyl adenylation reactions are typically reversible. An alternative explanation is that the pyrophosphate binding site is not accessible to solvent, as shown in the intermediate and product structures of  $\beta$ -LS (33), and an irreversible step, such as cyclization or a conformational change or product release, occurs after the formation of the distal acyl-AMP amino diacid intermediate.

In light of the ability of carbapenam synthetase to catalyze the ATP-dependent cyclization reaction of linear amino diacid compounds, such as L-amino adipic acid, the alternate substrates, glutaric, adipic, and pimelic acids, were used to investigate the formation of a distal acyl-AMP diacid intermediate. If the carbapenam reaction proceeds through a distal acyl-AMP amino diacid intermediate, the absence of the amino group involved in the intramolecular amide bond formation in the diacids would allow the reaction to proceed only to the distal acyl-AMP diacid intermediate. Hydroxamate formation and hydroxylamine-dependent AMP release have been considered evidence for the formation of acyladenylate intermediates in many enzymatic reactions (35). The dependence of AMP formation on the presence of both the diacid substrates and hydroxylamine, and the appearance of a characteristic chromophore after reacting with ferric chloride supports the existence of the proposed

Scheme 6



Scheme 7: Mechanism of the Carbapenam Synthetase Reaction



distal acyl-AMP amino diacid intermediate in the reaction catalyzed by carbapenam synthetase with CMPr (Scheme 7).

Surprisingly, PPi release was observed in the reaction with the diacids, and the distal acyl-AMP diacid intermediate was either released, or was accessible to hydroxylamine. In the absence of a crystal structure of carbapenam synthetase and considering the biochemical and sequence similarities with  $\beta$ -LS, the crystal structure of this latter enzyme may provide insights to interpret these results (33). In the substrate-bound structure of  $\beta$ -LS, the active site is open and accessible to solvent. Once the distal acyl-AMP amino diacid intermediate is formed, a conformational change occurs. The  $\beta$ -LS loop comprising residues 444–453, highly conserved in carbapenam synthetase as well, becomes ordered and blocks access to the active site. The PPi, therefore, is buried deep in a closed and protected active site and cannot diffuse out as was observed in the reaction with *N*<sup>2</sup>-(carboxymethyl)-L-arginine (23, 33). Similar conformational changes may occur in the reaction of carbapenam synthetase with CMPr where PPi is the last product to be released, but in the reactions with the diacids as substrates, the active site could remain in an open conformation allowing the distal acyl-AMP diacid

compound to diffuse into solution followed by the pyrophosphate.

Carbapenam synthetase shows broad substrate specificity. Remarkably, the effect on the turnover number by using different stereochemical analogues of CMPr in the carbapenam synthetase reaction is minimal. The increased  $K_m$  values and largely unchanged turnover rate constants are interpreted as caused by a weakened substrate affinity. Given the independence of the  $k_{cat}$  values on the stereochemistry at C-3 and C-5 of the substrate, one possibility is that another step in the mechanism, such as product release or a protein conformational change, rather than chemistry is partially rate limiting. Alternatively, if the chemistry is rate limiting, the in-line attack between the distal carboxylate and the  $\alpha$ -phosphoryl nonbridge oxygen of ATP and the subsequent cyclization step are not jeopardized by the different stereochemistries. Few or no specific interactions with the stereocenter at C-5 and with the carboxymethyl chain of CMPr in addition to free rotation around the C-6 and C-7 bond could account for the stereochemical promiscuity of the enzyme. The absence of electrostatic or hydrogen bond interactions with the carboxyl group at position 7 is also supported by the small decrease in substrate specificity observed in the reaction with CEP. In keeping with this interpretation, the crystal structure  $\beta$ -lactam synthetase with substrates bound reveals few contacts are formed between carboxyethyl-L-arginine, the second substrate, and the active site. No specific interactions occur at the carboxyethyl moiety of carboxyethyl-L-arginine (32), a common structural element between the substrates for  $\beta$ -lactam synthetase and carbapenam synthetase.

The lack of substrate specificity is highlighted by the ability of the enzyme to catalyze the cyclization reaction of different linear  $\alpha$ -amino diacids to five-, six-, and seven-membered lactam products. The decrease in the  $k_{cat}$  value observed in the reaction with D,L-aminopimelic acid is likely a consequence of unfavorable seven-membered ring formation. Accordingly, the faster reaction observed with CEP possibly owes to the ease of five-membered ring closure. The activity lost in  $k_{cat}$  in the reaction with L-glutamic acid can be accounted for by effects on the formation of the distal acyl-AMP amino diacid intermediate due to the shorter distance between the  $\alpha$ - and remote carboxylates. Favorable six-membered ring closure and similar separation between the two carboxylates can account for the minimal effect observed on  $k_{cat}$  in the reactions with D- and L-amino adipic acid. The dependence of the  $K_m$  values on the number of methylene groups present in the amino diacid substrates in addition to the absence of catalysis with carboxymethyl-aminopropionic acid and with the absence of catalysis and inhibition with L-aspartic acid suggests the presence of a hydrophobic pocket in the active site accommodating the methylenes at C-3, C-4, C-5, and C-6 of CMPr. The interactions with this hypothetical hydrophobic site would serve to position the substrate correctly for nucleophilic attack on ATP, and, hence, efficient catalysis. A spacer of at least two methylene groups between the  $\alpha$ - and remote carboxylates should be taken into account in the design of new substrates. The importance of the  $\alpha$ -carboxylate on substrate binding is revealed by the extremely weak inhibition shown by aminovaleric and aminocaproic acids. If instead of the  $\alpha$ -carboxylate the amino group is removed, the resulting



diacids are substrates of carbapenam synthetase. The amino group has little or no role in substrate binding as illustrated by the unchanged substrate specificity between one diacid compound and its corresponding amino diacid.

In conclusion, we have shown that carbapenam synthetase catalyzes in vitro the ATP-dependent intramolecular closure of CMP<sub>r</sub> to (3*S*,5*S*)-carbapenam-3-carboxylic acid. The kinetic mechanism is Bi-Ter where ATP is the first substrate to bind followed by CMP<sub>r</sub>, and PP<sub>i</sub> is the last product released. The reaction was shown to proceed through the formation of an acyladenylate intermediate followed by intramolecular amide bond formation. Carbapenam synthetase exhibits broad substrate specificity by catalyzing the formation of different sizes and stereochemistries of azobicyclic and monolactam products. The kinetic studies with alternate substrates and competitive inhibitors versus CMP<sub>r</sub> provide insights on the CMP<sub>r</sub> binding site and on which groups of the substrate are important for binding. While the amino group and distal carboxylate play little or no role in substrate binding, the  $\alpha$ -carboxylate is important for substrate affinity. We propose the presence of a hydrophobic pocket in the active site that interacts at least with the methylene groups of CMP<sub>r</sub>. While a more detailed explanation of these data awaits the acquisition of the three-dimensional structure of carbapenam synthetase, these results lay the foundation for future mechanistic studies. In addition, the alternate substrate binding data provided on the promiscuous carbapenam synthetase in combination with structural data will be useful in bioengineering studies on carbapenam synthetase aimed to improve antibiotic production and to biosynthesize novel  $\beta$ -lactam antibiotics.

## ACKNOWLEDGMENT

We are grateful to Prof. W. W. Cleland for critically reading this manuscript. We are thankful to Dr. Rongfeng Li for pET24a/*carA* plasmid and to Dr. Fumitaka Kudo for 3-(carboxymethylamino)-propionic acid.

## NOTE ADDED IN PROOF

Following submission of this manuscript, an article was published describing the identification and cloning of the thienamycin gene cluster from *S. cattleya* NRRL8057 (37).

## SUPPORTING INFORMATION AVAILABLE

Double-reciprocal plot of initial velocities, HPLC analysis of the reactions with glutamic and aminoadipic acid, and time course of AMP and PP<sub>i</sub> formation in the reaction with glutaric acid. Also included are the characterizations of each intermediate in the syntheses of alternate substrates, Ferguson plots obtained by native discontinuous electrophoresis and SDS-PAGE gel of fractions of carbapenam synthetase's purification. This material is available free of charge via the Internet at <http://pubs.acs.org>.

## REFERENCES

1. Kahan, J. S., Kahan, F. M., Goegelman, R., Currie, S. A., Jackson, M., Stapley, E. O., Miller, A. K., Hendlin, D., Mochales, S., Hernandez, S., Woodruff, H. B., and Birnbaum, J. (1979) *J. Antibiot.* 32, 1–12.
2. McGowan, S. J., Holden, M. T. G., Bycroft, B. W., and Salmond, G. P. C. (1999) *Antoine van Leeuwenhoek* 75, 135–141.
3. Bycroft, B. W., Maslen, C., Box, S. J., Brown, A., and Tyler, J. W. (1988) *J. Antibiot.* 41, 1231–1242.
4. Thomson, N. R., Crow, M. A., McGowan, S. J., Cox, A., and Salmond, G. P. C. (2000) *Mol. Microbiol.* 36, 539–556.
5. McGowan, S. J., Sebahia, M., Porter, L. E., Stewart, G. S. A. B., Williams, P., Bycroft, B. W., and Salmond, G. P. C. (1996) *Mol. Microbiol.* 22, 415–426.
6. Derzelle, S., Duchaud, E., Kunst, F., Danchin, A., and Bertin, P. (2002) *Appl. Environ. Microbiol.* 68, 3780–3789.
7. McGowan, S. J., Sebahia, M., O'Leary, S., Hardie, K. R., Williams, P., Stewart, G. S. A. B., Bycroft, B. W., and Salmond, G. P. C. (1997) *Mol. Microbiol.* 26, 545–556.
8. Li, R., Stapon, A., Blanchfield, J. T., and Townsend, C. A. (2000) *J. Am. Chem. Soc.* 122, 9296–9297.
9. Stapon, A., Li, R., and Townsend, C. A. (2003) *J. Am. Chem. Soc.*, in press.
10. Akasaka, K., Akamatsu, H., Kimoto, Y., Shimizu, T., Shimomura, N., Tagami, K., and Negi, S. (1999) *Chem. Pharm. Bull.* 47, 1525–1531.
11. Bycroft, B. W., Maslen, C., Box, S. J., Brown, A., and Tyler, J. W. (1988) *J. Antibiot.* 41, 1231–1242.
12. Kolasa, T., and Miller, M. J. (1990) *J. Org. Chem.* 55, 1711–1721.
13. Barrett, A. G. M., Head, J., Smith, M. L., Stock, N. S., White, A. J. P., and Williams, D. J. (1999) *J. Org. Chem.* 64, 6005–6018.
14. Ezquerro, J., and Pedregal, C. (1994) *Tetrahedron Lett.* 35, 2053–2056.
15. Collado, I., Ezquerro, J., Vaquero, J. J., and Pedregal, C. (1994) *Tetrahedron Lett.* 35, 8037–8040.
16. Petersen, J. S. F. G., and Rapoport, H. (1984) *J. Am. Chem. Soc.* 106, 4539–4547.
17. Aoki, H., Kubochi, Y., Iguchi, E., and Imanaka, H. (1976) *J. Antibiot.* 29, 492–500.
18. Van Pelt, J. E., and Northrop, D. B. (1984) *Arch. Biochem. Biophys.* 230, 250–263.
19. Hegeman, A. D., Gross, J. W., and Frey, P. A. (2001) *Biochemistry* 40, 6598–6610.
20. Jaworek, D., Gruber, W., and Bergmeyer, H. U. (1974) in *Methods of Enzymatic Analysis* (Bergmeyer, H. U., and Gawehn, K., Eds) 2nd ed., Vol. 4, pp 2127–2129, Academic Press, Inc., New York.
21. Cleland, W. W. (1979) *Methods Enzymol.* 63, 103–138.
22. Anderson, P. M., and Meister, A. (1966) *Biochemistry* 5, 3157–3163.
23. Bachmann, B. O., and Townsend, C. A. (2000) *Biochemistry* 39, 11187–11193.
24. Ferguson, K. A. (1964) *Metabolism* 13, 985–1002.
25. Gensmantel, N. P., Proctor, P., and Page, M. I. (1980) *J. Chem. Soc., Perkin Trans. 2*, 1725–1732.
26. Mendez, R., Alemany, T., and Martin-Villacorta J. (1992) *Chem. Pharm. Bull.* 40, 3228–3233.
27. Stadtman, E. R. (1957) *Methods Enzymol.* 3, 228–231.
28. Hsu, R. Y., Lardy, H. A., and Cleland, W. W. (1967) *J. Biochem.* 242, 5315–5322.
29. Jencks, W. P. (1957) *Biochim. Biophys. Acta* 24, 227–228.
30. Duclos, B., Maracandier, S., and Cozzzone, A. J. (1991) *Methods Enzymol.* 201, 10–21.
31. Larsen, T. M., Boehlein, S. K., Schuster, S. M., Richards, N. G. J., Thoden, J. B., Holden, H. M., and Rayment, I. (1999) *Biochemistry* 38, 16146–16157.
32. Miller, M. T., Bachmann, B. O., Townsend, C. A., and Rosenzweig, A. C. (2001) *Nat. Struct. Biol.* 8, 684–689.
33. Miller, M. T., Bachmann, B. O., Townsend, C. A., and Rosenzweig, A. C. (2002) *Proc. Natl. Acad. Sci. U.S.A.* 99, 14752–14757.
34. Bachmann, B. O., Li, R., and Townsend, C. A. (1998) *Proc. Natl. Acad. Sci. U.S.A.* 95, 9082–9086.
35. Boehlein, S. K., Stewart, J. D., Walworth, E. S., Thirumoorthy, R., Richards, N. G. J., and Schuster, S. M. (1998) *Biochemistry* 37, 13230–13238.
36. Stadtman, E. R. (1973) *The Enzymes* (Boyer, Ed.) Vol. 8, pp 1–11, Academic Press, New York.
37. Núñez, L. E., Méndez, C., Braña, A. F., Blanco, G., and Salas, J. A. (2003) *Chem. Biol.* 10, 301–311.